Development of Peltate Glandular Trichomes of Peppermint[1]

Glenn W. Turner, Jonathan Gershenzon[2], and Rodney B. Croteau*

Institute of Biological Chemistry, Washington State University, Pullman, Washington 99164–6340

Cryofixation and conventional chemical fixation methods were employed to examine the ultrastructure of developing peltate glandular trichomes of peppermint (*Mentha* × *piperita*). Our results are discussed in relation to monoterpene production and the mechanism of essential oil secretion. Peltate glands arise as epidermal protuberances (initials) that divide asymmetrically to produce a vacuolate basal cell, a stalk cell, and a cytoplasmically dense apical cell. Further divisions of the apical cell produce a peltate trichome with one basal cell, one stalk cell, and eight glandular (secretory) disc cells. Presecretory gland cells resemble meristematic cells because they contain proplastids, small vacuoles, and large nuclei. The secretory phase coincides with the separation and filling of the sub-cuticular oil storage space, the maturation of glandular disc cell leucoplasts in which monoterpene biosynthesis is known to be initiated, and the formation of extensive smooth endoplasmic reticulum at which hydroxylation steps of the monoterpene biosynthetic pathway occur. The smooth endoplasmic reticulum of the secretory cells appears to form associations with both the leucoplasts and the plasma membrane bordering the sub-cuticular oil storage cavity, often contains densely staining material, and may be involved with the transport of the monoterpene-rich secretion product. Associated changes in the ultrastructure of the secretory stage stalk cell are also described, as is the ultrastructure of the fragile post-secretory gland for which cryofixation methods are particularly well suited for the preservation of organizational integrity.

Monoterpenes (C_{10}) comprise the major components of the essential oils of the mint family (Lamiaceae), including peppermint (*Mentha* × *piperita*), which has been developed as a model system for the study of monoterpene metabolism. Peppermint oil is chemically complex and the biosynthetic pathway leading to the major component (−)-menthol (Fig. 1) involves essentially all of the representative reaction types of terpenoid metabolism (Croteau and Gershenzon, 1994). Monoterpene biosynthesis and accumulation in mint has been specifically localized to the glandular trichomes (Gershenzon et al., 1989; McCaskill et al., 1992). The pathway originates in the plastids (leucoplasts) of the secretory cells of these highly specialized, non-photosynthetic glandular structures (Turner et al., 1999) because both the universal acyclic precursor geranyl diphosphate (Burke et al., 1999) and the first committed intermediate of the pathway (−)-limonene (Kjonaas and Croteau, 1983; Colby et al., 1993; Turner et al., 1999) are now known to arise from primary metabolism at this locale. The first cyclic intermediate (−)-limonene subsequently undergoes cytochrome P450-catalyzed hydroxylation to (−)-trans-isopiperitenol at the endoplasmic reticulum (ER) (Karp et al., 1990; Lupien et al., 1999), and the remaining transformations, comprising largely redox metabolism (Fig. 1), appear to occur in the cytosol (Wise and Croteau, 1999).

With the pathway for the biosynthesis of peppermint monoterpenes and the subcellular locations of the various steps defined, more recent attention has turned to the regulation of metabolism of these constitutively produced natural products. Developmental and environmental factors are both known to markedly influence the yield and composition of peppermint oil, with obvious consequences for the commercial production of this commodity (Burbott and Loomis, 1967; Clark and Menary, 1980); however, the means by which these variables exert regulatory control over pathway flux or the specific steps of monoterpene metabolism are not fully clear. Studies at the level of the intact plant have indicated that monoterpene production (measured by incorporation of $^{14}CO_2$) is restricted to young leaves 12 to 20 d of age (prior to full leaf expansion) and that metabolic turnover of oil components (Mihaliak et al., 1991) and evaporative losses of oil from the storage compartment play only minor roles in determining oil yield and composition (Gershenzon et al., 2000). These results, combined with the lack of evidence for the control of pathway enzyme activity by allosteric modulation or covalent modification (Wise and Croteau, 1999), suggest that oil composition and yield might reflect the simple kinetic consequences of the levels of biosynthetic enzymes present, as determined by transcriptional and translational production of these pathway catalysts and their subsequent turnover.

[1] This work was supported in part by the U.S. Department of Energy Division of Energy Biosciences, the Mint Industry Research Council, and the Agricultural Research Center, Washington State University (project no. 0268).

[2] Present address: Max Planck Institut für Chemische Ökologie, Tatzendpromenade 1a, D–07745 Jena, Germany.

* Corresponding author; e-mail croteau@mail.wsu.edu; fax 509–335–7643.

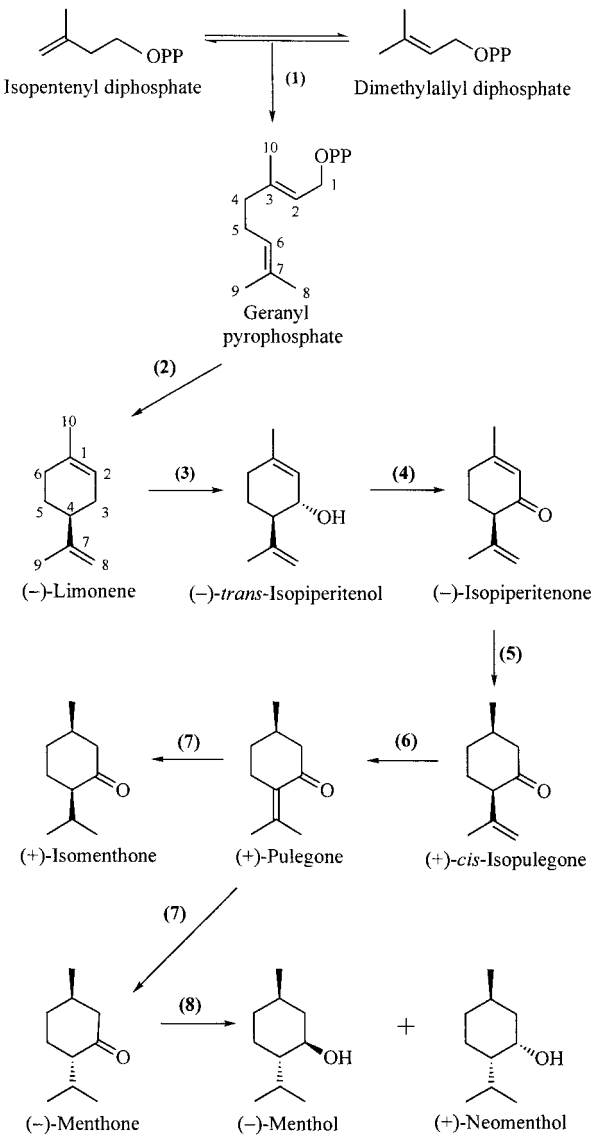

Figure 1. The principal pathway for monoterpene biosynthesis in peppermint. The responsible enzymes are: geranyl diphosphate synthase (1), (4*S*)-(−)-limonene synthase (2), cytochrome P450 (−)-limonene-3-hydroxylase (3), (−)-trans-isopiperitenol dehydrogenase (4), (−)-isopiperitenone reductase (5), (+)-cis-isopulegone isomerase (6), (+)-pulegone reductase (7), and (−)-menthone reductase (8).

Using oil glands isolated from peppermint leaves of different ages, in vitro assays of the eight sequential enzymes responsible for the biosynthesis of (−)-menthol (Fig. 1) have now shown that all but (−)-menthone reductase (Kjonaas et al., 1982) have a very similar developmental profile, with high levels of activity in leaves 12 to 20 d of age and a sharp peak of activity centered at 15 d (McConkey et al., 2000). This correlation between in vitro enzyme activity and the rate of biosynthesis measured in vivo suggests that monoterpene formation is controlled by the coordinately regulated activity of the relevant biosynthetic enzymes. Developmental immunoblotting of limonene synthase demonstrated a direct correlation between enzyme activity and enzyme protein, and RNA-blot analyses indicated that the genes encoding the monoterpene biosynthetic enzymes are transcriptionally activated in a coordinated fashion, with a time course that can be superimposed on activity measurements and immunoblot data (McConkey et al., 2000). These results demonstrate coincidental temporal changes in enzyme activities, enzyme protein level, and steady-state transcript abundances and indicate that most of the monoterpene biosynthetic enzymes in peppermint oil glands are developmentally regulated at the level of gene expression.

In the preceding paper (Turner et al., 2000), the population dynamics of peltate glandular trichome development on expanding peppermint leaves were described. These data, in addition to defining the developmental patterns of peltate gland initiation and ontogeny as these structures produce eight secretory cells and commence filling of the subcuticular oil storage cavity, have also demonstrated that the maximum monoterpene production rates determined previously by in vivo (Gershenzon et al., 2000) and in vitro (McConkey et al., 2000) time-course studies correlate directly with the number of leaf oil glands present in the secretory stage of development. Moreover, it was shown that gland development is a very rapid process (approximately 60 h) with respect to leaf expansion (18–25 d), with the progression from initiation to secretory phase taking 30 h and the gland-filling process itself requiring less than 30 h. An understanding of oil gland structure and function is necessary to fully evaluate the regulation of monoterpene biosynthesis and might elucidate the means of metabolite trafficking between the various organellar sites and the mechanics of secretion (export) of essential oil to the sub-cuticular storage depot, processes about which virtually nothing is presently known. Considering the importance of this functional understanding, and the economic significance of essential oils from the Lamiaceae, there have been surprisingly few studies of gland ultrastructure in these species (Amelunxen, 1965; Bosabalidis and Tsekos, 1982; Heinrich et al., 1983; Bourett et al., 1994; Ascensão et al., 1997). Of these, only Amelunxen (1965) reported on peppermint gland ultrastructure, but this early study employed OsO_4 as the sole fixative and preservation of the ultrastructure appears to have been severely compromised.

In the present study, we employed high-pressure freezing and freeze-substitution (HPFS), rapid microwave oven fixation (Giberson et al., 1997), and conventional chemical fixation to preserve gland cells for microscopy. Cryofixation in particular stabilizes tissue ultrastructure very rapidly (<10 ms), thereby eliminating many artifacts encountered with conventional fixation methods (Hayat, 1989; Galway et al.,

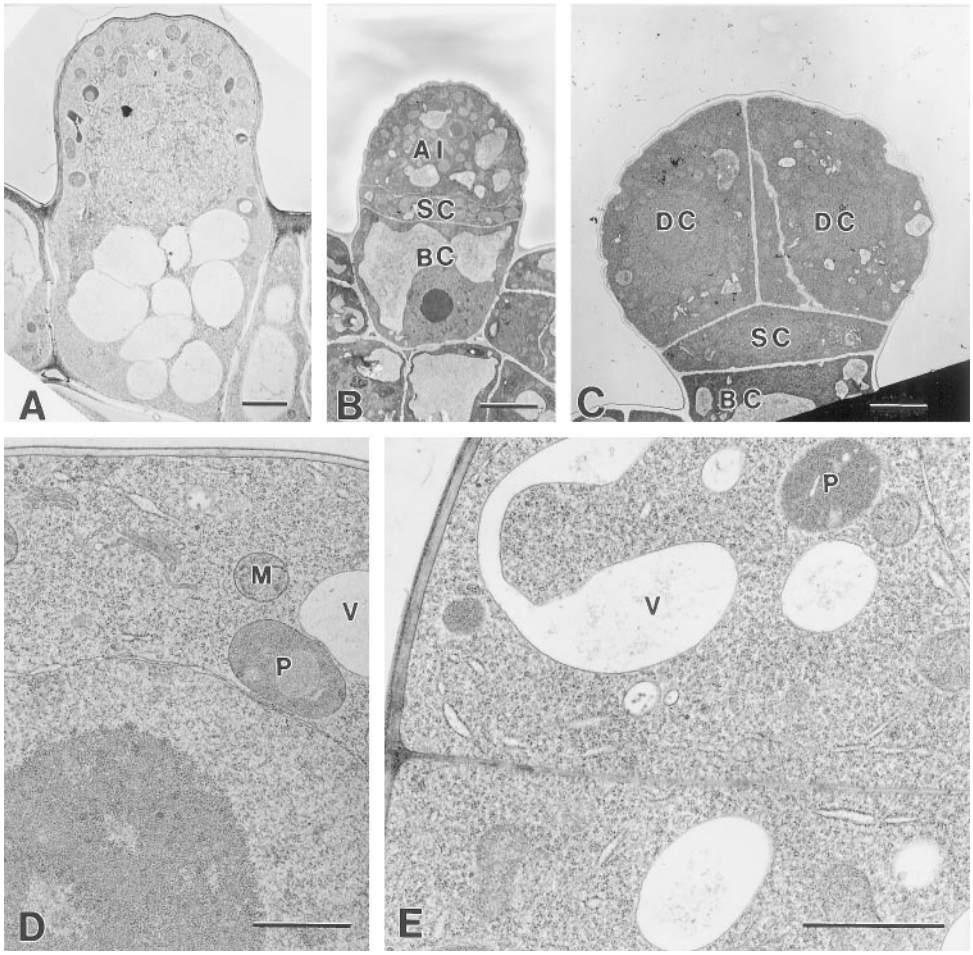

Figure 2. Early presecretory stage. A, Cryofixed glandular trichome initial consisting of a single cell with a vacuolate basal region and an apical region containing the nucleus, numerous mitochondria, and plastids, but few vacuoles. Bar = 2 μm. B, Chemically fixed glandular trichome initial after periclinal cell divisions, with a vacuolate basal cell (BC), narrow stalk cell (SC), and the apical disc initial cell (AI). Bar = 5 μm. C, Chemically fixed developing peltate glandular trichome with four apical disc cells (DC). Bar = 4 μm. D, Cryofixed apical initial of a developing glandular trichome with a single apical cell. The nucleus and nucleolus are large and the ribosomes are abundant but ER is relatively sparse. P, Proplastid; M, mitochondrion; V, vacuole. Bar = 1 μm. E, Periclinal section through a cryofixed, two-celled, apical disc. P, Proplastid; V, vacuole. Bar = 1 μm.

1995; Parthasarathy, 1995). The results described here provide essential structural context for our previous biosynthetic and regulatory studies (Gershenzon et al., 2000; McConkey et al., 2000), suggest roles for leucoplasts and smooth ER (SER) in essential oil production and secretion, and indicate that some artifacts of standard fixation methods have been very misleading, especially in relation to the structure of post-secretory glands.

RESULTS

Initiation of Glandular Trichomes

Capitate and peltate glandular trichomes of peppermint cannot be easily distinguished at their inception. Both are first discernible as protruding epidermal cells with an asymmetrical cytoplasmic distribution containing vacuolate basal portions and cytoplasmically dense apical portions (Fig. 2A). Trichomes that are slightly older are partitioned by periclinal cell divisions separating an apical initial, a narrow stalk cell, and a vacuolate basal cell (Fig. 2B). In developing peltate glands, three sets of anticlinal cell divisions follow in the apical disc (Figs. 2C and 3, A and B), eventually producing an eight-celled apical disc (Fig. 4A).

Presecretory Stage

The presecretory stage includes all developmental phases prior to the inception of gland filling. This stage is a time of cell division and growth during which peltate glands produce eight glandular cells

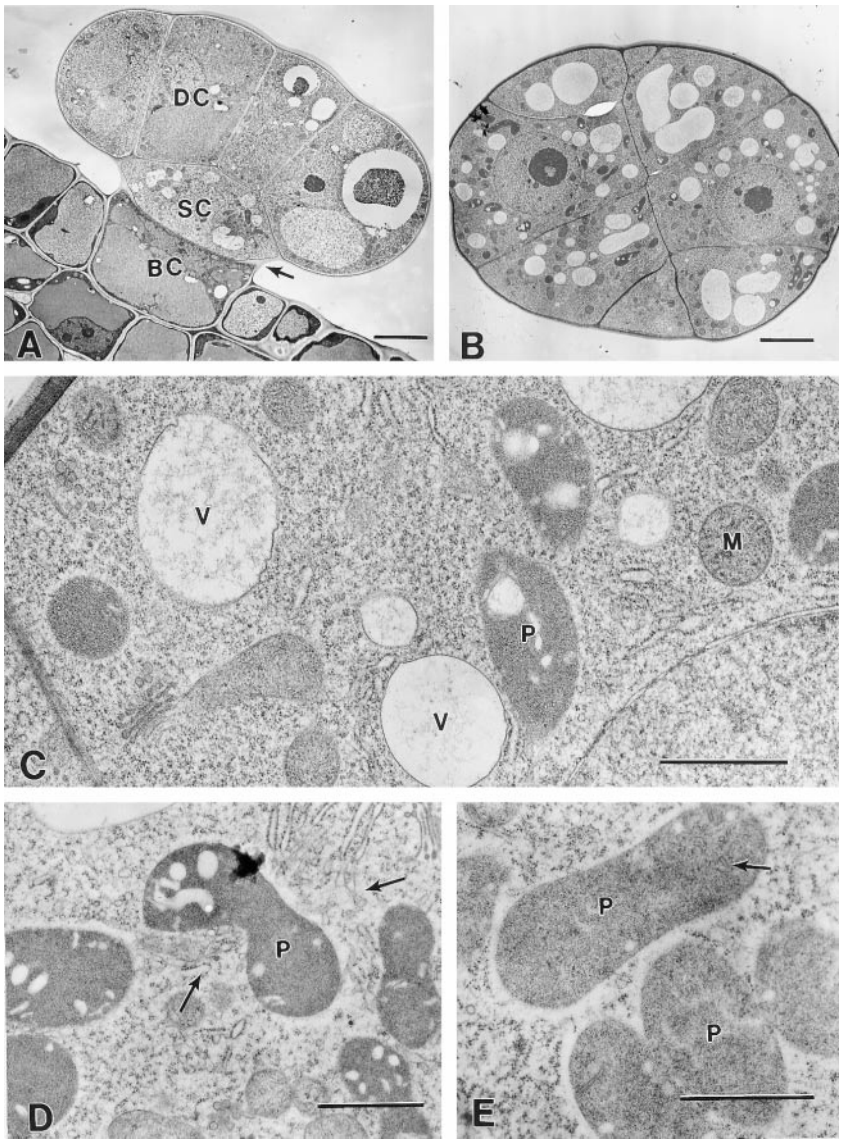

Figure 3. Middle- to late-presecretory stage. A, Transverse section through a chemically fixed presecretory peltate gland with an eight-celled apical disc. BC, Basal cell; SC, stalk cell; DC, disc cell. Arrow indicates a thickening stalk cell lateral wall. Bar = 5 mm. B, Periclinal section through a cryofixed apical disc of a presecretory stage gland. Bar = 5 μm. C, Higher magnification of the specimen shown in (B). The disc cells appear typical of developing plant cells with numerous ribosomes, small vacuoles (V), abundant Golgi, mitochondria (M), and small proplastids (P). Bar = 1 μm. D, Cryofixed apical disc cells of a late-presecretory gland. SER (arrows) is relatively abundant near the enlarging plastids (P). Bar = 1 μm. E, Cryofixed stalk cell of a late-presecretory stage gland. Plastids (P) remain relatively narrow and contain numerous tubular membranes (arrow). Bar = 1 μm.

and reach their full size. Glandular disc cells from presecretory glands ultrastructurally resemble meristematic cells, with few small vacuoles, relatively large nuclei, large nucleoli, numerous ribosomes, and proplastids. At early stages, the proplastids are small and the ER is relatively sparse but, as the glands become larger, plastids appear larger and rough ER (RER) becomes more abundant (Fig. 2, D and E; Fig. 3, C and D). During the middle and late presecretory stages, the plastidome consists of amoeboid proplastids that often contain moderately large plastoglobuli and peripheral tubular membranes (Fig. 3, C and D). Golgi are common in glandular disc cells. Disc cells of the last presecretory stage (Fig. 3D) contain both regions of well-developed RER and SER, which is especially abundant near plastids (Fig. 3D). The distal cell walls at the apex of a gland develop a thickened cuticle prior to the secretory phase (Fig. 3A). This thickening is greatest at the gland apex, where the cuticle appears to be about twice as thick as that covering the lateral sides of the gland. The cuticle averaged 0.2 μm in thickness on small glands of the early presecretory stage and 0.7 μm in thickness at the apex of late presecretory glands.

During the presecretory phase, glandular trichome stalk cells contain relatively small vacuoles, large nuclei with large nucleoli, numerous mitochondria, and proplastids that lack large plastoglobuli. Microbodies are rare in presecretory stalk cells, Golgi are common, and there is a well-developed RER. Plasmodesmata are abundant in the cell walls bordering the glandular disc cells and basal cell. The lateral wall of the stalk cell (forming a boundary to the exterior) thickens and shows some evidence of suberization relatively early in gland development (by the four-disc cell stage).

By the final presecretory stage, the stalk cell plastids are still variable in shape and somewhat elon-

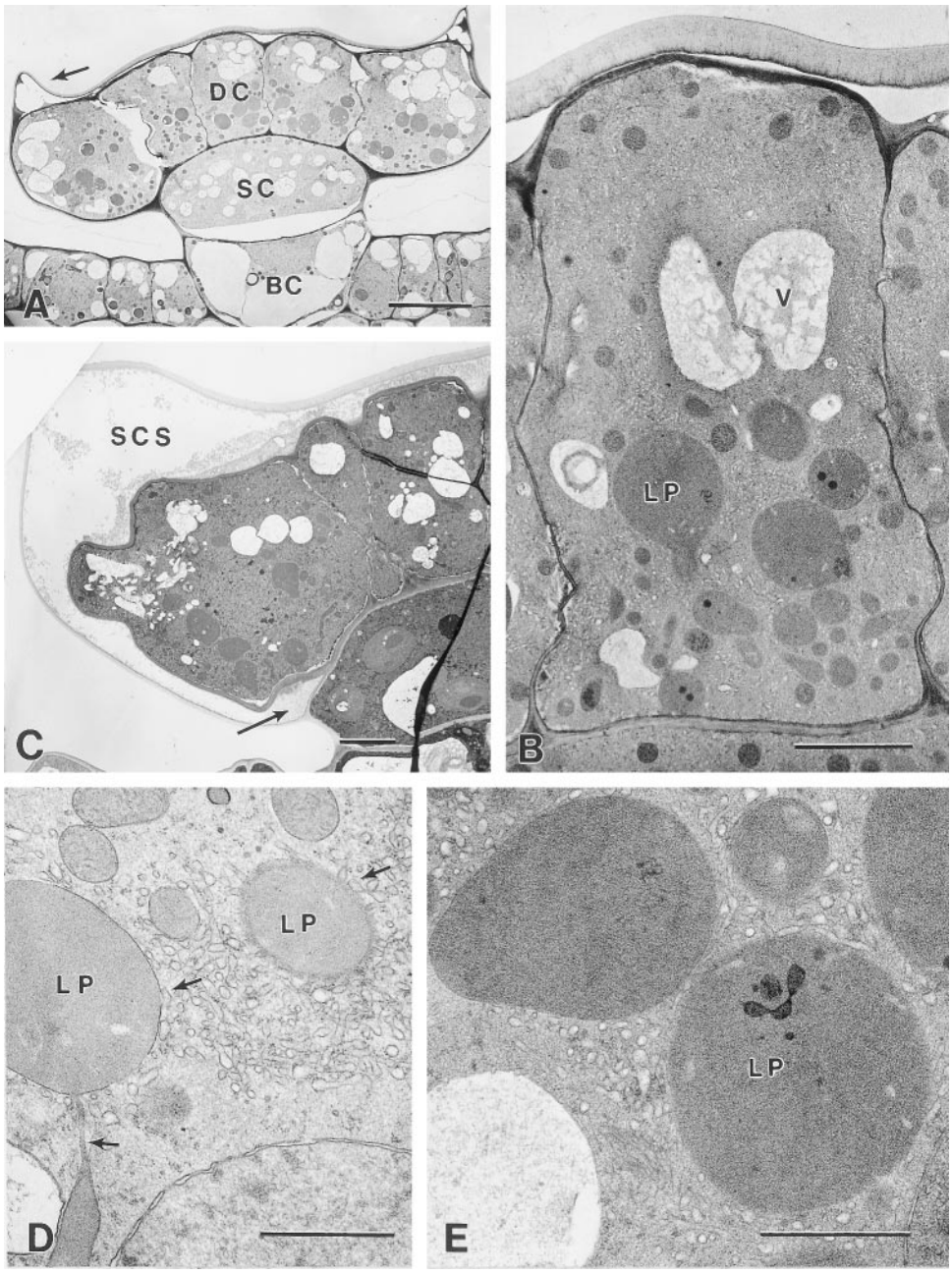

Figure 4. Secretory stage. A, Cryofixed early-secretory stage peltate gland. DC, Apical disc cell; SC, stalk cell; BC, basal cell. Arrow indicates the lateral rim of raised cuticle. Bar = 10 μm. B, Cryofixed apical disc cell of a secretory stage peltate gland. Large leucoplasts (LP) occur mainly in the basal one-half of the cell. An extensive SER occurs throughout the cell, except near vacuoles (V). Lateral disc cell walls remain thin and have become densely staining. Bar = 3 μm. C, Chemically fixed secretory stage peltate gland. Arrow indicates the lowermost extension of the sub-cuticular oil storage space (SCS) at the juncture of the stalk and disc cells. Bar = 5 μm. D, Portion of a cryofixed disc cell showing leucoplasts (LP) in close contact with SER. Upper arrows indicate apparent contact between SER and plastid membranes. The structure indicated by the lower arrow is a narrow portion (near the edge) of a leucoplast branch. Bar = 1 μm. E, Cryofixed leucoplasts (LP) of a secretory stage gland in close contact with SER. Bar = 1 μm.

gated, but contain numerous tubular membranes throughout the stroma (Fig. 3E). Late presecretory-stage stalk cells contain regions of well-developed RER and SER and numerous mitochondria and Golgi, but microbodies are rare.

Basal cells of presecretory glands remain vacuolate, and their peripheral cytoplasm appears to contain fewer organelles than the stalk or disc cells. The plastids are small, often appear roughly spherical, and have large plastoglobuli relative to the plastid

volume. Mitochondria are common, and the ER is well developed, consisting mostly of RER.

Secretory Stage

Secretory stage glandular disc cells are characterized by enlarged leucoplasts, an extensive SER, and the detachment of the thick cuticle from the outer cell walls to form an extensive extracellular SCS. During the secretory stage, the distributions of leucoplasts, SER, vacuoles, and lipid deposits of the glandular disc cells exhibit distinct zonation. The stalk cells also undergo evident changes during the secretion stage in developing large, unusual plastids, an extensive SER, and numerous microbodies.

Onset of the secretory phase is marked by separation of the thickened cuticle across the apical surface of the gland (Fig. 4, A–C). After separation, the gland cuticle is bordered on the lower surface (adjacent to the sub-cuticular cavity) by a thin, uniform, darkly staining layer that probably represents a layer of cell wall (Figs. 4B and 5D). The cuticle initially remains attached to the lateral walls of the glandular disc (secretory) cells, but the cuticular separation soon spreads, extending to the stalk cell-disc cell juncture where the lateral stalk cell wall becomes permeated with lightly staining, suberin-like material (compare Fig. 4A with Fig. 4C). The stalk cell and secretory disc cells separate over a short distance above a terminal extension of this suberized region in the distal stalk cell wall, forming a short extension of the subcuticular space in contact with the stalk cell (Fig. 4C).

Radial walls of the secretory cells often stain darkly, remain remarkably thin, and form undulating boundaries with occasional plasmodesmata. Treatment with pectinase revealed that the walls of these cells are rich in pectin but also contain a matrix of cellulose microfibrils. Plasmodesmata often traverse both the disc cell-stalk cell boundary and the cell walls separating the stalk and basal cells.

Mature plastids of the secretory stage disc cells are typical of the secretory gland leucoplasts previously observed in the Lamiaceae (Bosabalidis and Tsekos, 1982; Cheniclet and Carde, 1985; Ascensão et al., 1997). These plastids are found only in secretory disc cells, usually in the basal one-half of the cells (adjacent to the stalk cell); the distal portion of the disc cells contains most of the vacuoles (Fig. 4, A and B). These leucoplasts are variable in form but often have a large central body with a number of narrow branches. These leucoplasts lack chlorophyll, grana, and starch grains, and have a sparse network of tubular internal membranes, small plastoglobuli, and an amorphous stroma that is uniformly densely staining (Fig. 4, D and E). Ribosome-sized particles are found sparsely scattered within cryofixed leucoplasts. The internal plastid membranes are often observed near the plastid periphery. The leucoplasts are surrounded by SER that closely approaches the outer plastid membrane and often appears to be in direct contact with the membrane (Fig. 4D). This periplastic SER remains associated with plastids even near vacuoles where SER elements are relatively rare. In microwave-fixed specimens, periplastic SER often contains lipid deposits (Fig. 5K).

Proper membrane staining of microwave-fixed glandular disc cells proved to be difficult, and membranes were poorly differentiated with uranyl acetate staining. Some microwave-fixed specimens (Fig. 5, G and I–K) were stained with a neutral solution of phosphotungstinate. This staining provided adequate contrast to membranes and revealed darkly stained deposits within the SER. Although phosphotungstinate will stain a variety of compounds, including carbohydrates and proteins, it is likely that the darkly stained material shown in these figures (Fig. 5, F and I–K) represents lipid because, when stained with uranyl acetate, it appeared as a light-gray shade (typical of lipid) and it exhibited similar staining density to fixed material in the SCS. This material almost certainly represents essential oil because like the oil of the storage space, it was removed during freeze substitution.

The SER forms an extensive network throughout the disc cells and is especially abundant in the apical one-half of the cells near the sub-cuticular essential oil storage space (Figs. 4B and 5B). Small vesicles, enclosed by SER, also occur in this region. These vesicles appear empty in samples prepared by freeze substitution (Figs. 5B and 5H), but consistently contain lipid-like material in specimens fixed by the microwave method (Fig. 5I).

The ER is predominantly smooth and tubular but polysomes are frequently attached to scattered regions throughout (Figs. 4D and 5, A and C). In microwave-fixed tissues, lipid-like material occurs throughout the SER in short segments (Fig. 5, G and I–K). There is an evident polarity to this distribution, with more darkly staining deposits near the SCS than in the basal regions of the secretory cells. Osmiophilic deposits are consistently present along lateral walls near the SCS (for about one-third of cell height below the apex), but are absent from the basal portions of the same cell walls (Fig. 5G). Similar electron-dense material often partially fills the small vacuoles in the apical one-half of the secretory cells.

SER appears to closely approach or contact the plasma membrane and is aligned as parallel tubes along the radial and distal cell walls. This phenomenon can be seen along the radial cell wall in Figure 5A, and in Figure 5, B and C, where a glancing section through the distal wall exposes an array of closely aligned SER approaching the plasma membrane. In microwave-fixed glandular disc cells, similar regions of cortical SER often contain lipid deposits (Fig. 5J).

Two distinct materials accumulate in the subcuticular storage space during the secretory phase: A

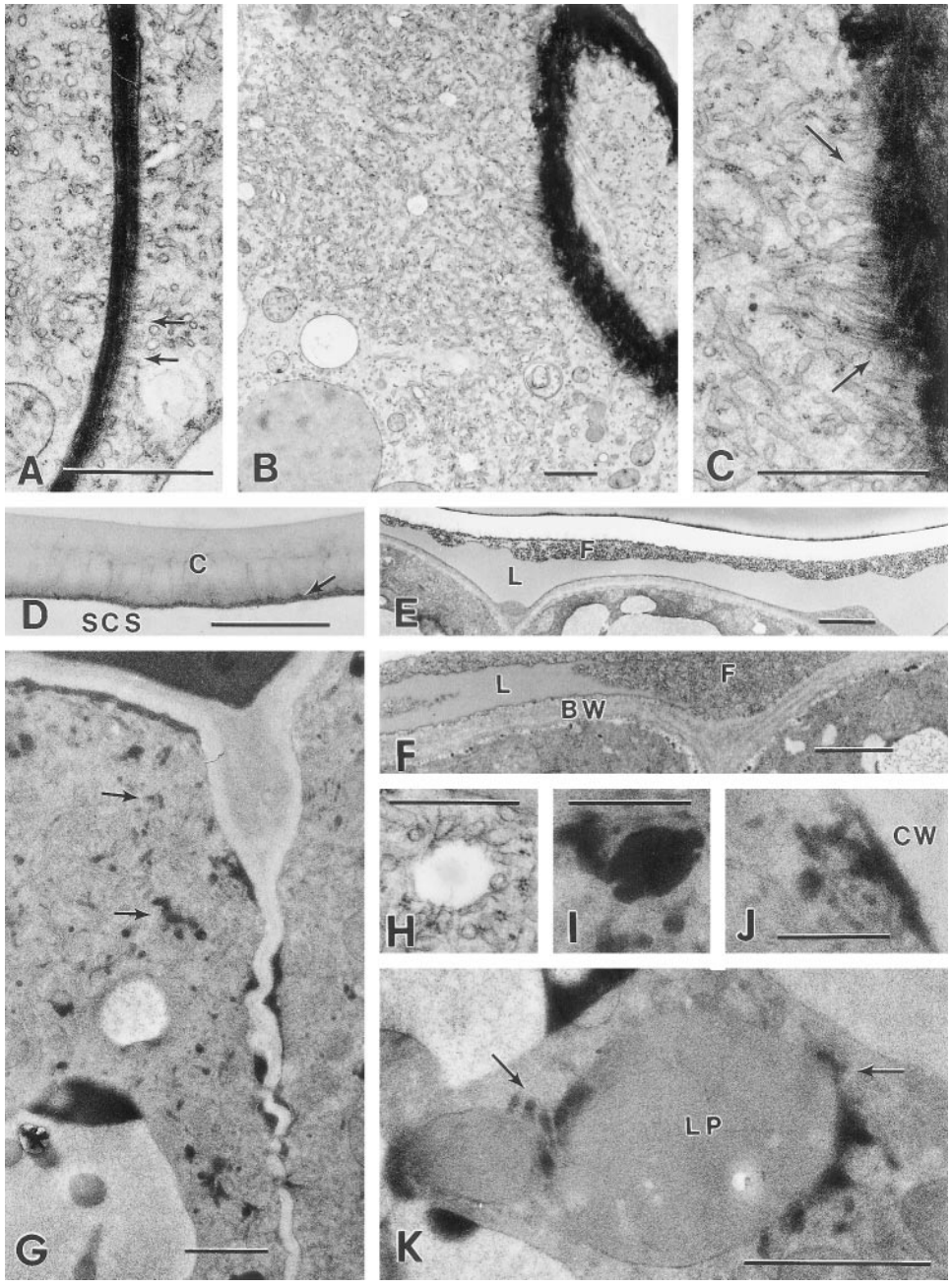

Figure 5. Secretory stage. A, SER adjacent to a densely staining radial wall of a cryofixed disc cell showing the apparent alignment of the SER along the plasma membrane (arrows). Bar = 1 μm. B, Extensively developed SER in a cryofixed secretory stage disc cell, near a glancing section through the boundary wall bordering the sub-cuticular storage space (upper right). Bar = 1 μm. C, Higher magnification of (B) showing the alignment of SER adjacent to the plasma membrane along the boundary wall (arrows). Bar = 1 μm. D, Elevated cuticle (C) at the apex of a cryofixed secretory stage gland. Arrow indicates a thin layer of residual cell wall. Bar = 1 μm. E, Sub-cuticular storage space in the apical region of a chemically fixed early secretory stage peltate gland containing lipid-like material (L) and fibrillar material (F). Bar = 2 μm. F, Higher magnification of a sub-cuticular region of a chemically fixed peltate gland showing layers of lipid-like material (L) within the fibrillar matrix (F) near the disc cell boundary cell wall (BW). Bar = 1 μm. G, Microwave-fixed glandular disc cells of a secretory phase peltate gland. Note the dark lipid-like deposits within the SER (arrows) and along the lateral cell walls. Bar = 1 μm. H, Vesicle-like structure in close contact with SER of a cryofixed glandular disc cell. Equivalent structures in microwave-fixed tissues consistently contain osmiophilic material. Compare with (I). Bar = 0.5 μm. I, Lipid-containing vesicle in close contact with SER of a microwave-fixed glandular disc cell. Bar = 0.5 μm. J, Enlargement of (G) showing a lipid-filled region of SER in close contact with the plasma membrane along the lateral cell wall (CW). Bar = 0.5 μm. K, Leucoplast (LP) from a microwave-fixed glandular disc cell in close contact with lipid-filled periplastic SER (arrows). Bar = 1 μm.

smooth-textured, osmiophilic material comprises most of the cavity volume (and is presumably essential oil) and another, apparently hydrophilic, material forms a relatively thin coating over the secretory cells and is evidently distinct from the cell walls (Figs. 4C and 5F). With chemical fixation, the latter material often appears fibrillar. In freeze-substituted samples, which generally lose the stored oil, the corresponding material appears as a thick amorphous layer that lacks fine fibrils but sometimes contains many small pockets. In some preparations of secretory stage glands, a smooth-textured, lipid-like material occurs within the fibrillar substance, either as small droplets or as thin, sheet-like layers (Fig. 5, E and F).

Each of the eight disc cells is attached on the lower surface to a single, broad, and convex stalk cell, which in turn is attached to a single basal cell. Secretory-stage stalk cells differ from stalk cells of presecretory glands because they contain unusual plastids, an extensive SER, numerous mitochondria, numerous microbodies, and heavily suberized lateral walls (Fig. 6, B–E).

The periclinal walls of the stalk cell, the distal wall bordering the eight secretory disc cells, and the lower wall bordering the basal cell contain plasmodesmata. The lateral anticlinal cell wall forms a boundary to the exterior and is heavily suberized (Fig. 4, A and C). This cell wall appears to be brittle because occasionally lateral stalk cell walls are fractured during tissue processing, and it is at this location that breakage occurs when disc cell clusters are isolated by a leaf surface abrasion technique (Gershenzon et al., 1992).

Stalk cells contain numerous, large, nearly spherical, and unbranched plastids with densely staining stroma (Fig. 6, A and B). Stalk cells often contain a large plastoglobule placed to one side and a prolamellar body-like, crystaloid membrane structure at the opposite side of the plastid (Fig. 6, C and D). Solitary, thylakoid-like membranes often occur adja-

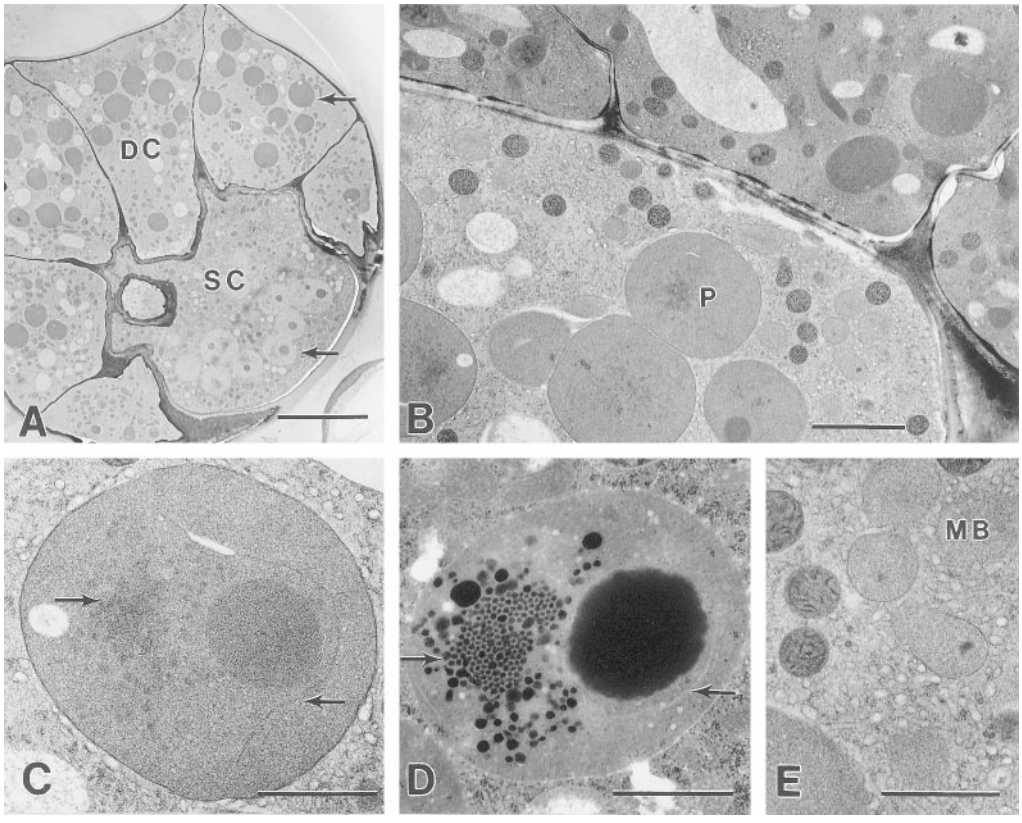

Figure 6. A, Peridermal section through glandular disc cells (DC) and the stalk cell (SC) of a cryofixed secretory stage peltate gland. Leucoplasts (upper arrow) of disc cells stain darkly and have few plastoglobuli, whereas stalk cell plastids (lower arrow) stain lightly and have large plastoglobuli. Bar = 10 μm. B, Transverse section through a cryofixed secretory stage gland. The stalk cell contains large plastids (P), abundant SER, numerous darkly staining mitochondria, and numerous lightly stained microbodies. Bar = 2 μm. C, Typical stalk cell plastid from a cryofixed gland. The left arrow indicates a small prolamellar body-like region of crystaloid plastid membranes. The right arrow indicates an isolated membrane forming a pocket around the large plastoglobule. Bar = 1 μm. D, Typical glandular stalk cell plastid from a chemically fixed peltate gland showing a similar prolamellar body-like region (arrow), and an isolated membrane enclosing a large plastoglobule. Compare with (C). Bar = 1 μm. E, Microbodies (MB) surrounded by an extensive SER in the stalk cell of a cryofixed secretory stage gland. Bar = 1 μm.

cent to the large plastoglobule (Fig. 6C). With standard chemical fixation, the polygonal spaces between prolamellar body-like membranes were observed to be filled with darkly staining osmiophilic material, and small plastoglobuli occurred in the surrounding stroma (Fig. 6D). Freeze-substituted specimens showed similar plastid structure but with the loss of densely staining lipid-like material (Fig. 6C). Like the disc cell leucoplasts, the stalk cell plastids often make close contact with surrounding SER (Fig. 6C).

The basal cell of secretory stage glands retains a large central vacuole. The periclinal cell wall, bordering the stalk cell, usually contains branched plasmodesmata. The peripheral cytoplasm contains abundant SER. Plastids of the basal cell are much smaller and less abundant than disc cell or stalk cell plastids. They also lack grana, have dense stroma, possess some tubular internal membranes, and often contain large plastoglobuli. Mitochondria are common in secretory stage basal cells but appear to be less abundant than in stalk and disc cells. Microbodies were not observed.

Post-Secretory Stage

Post-secretory glands with filled SCSs appear as ovoid domes in slight depressions of the mature leaf epidermis (Fig. 7A). In fixed tissues, the domes are often partially collapsed, or appear somewhat flat-topped but in fresh, unfixed, specimens, the domes are clearly rounded due to internal pressure from the stored secretion. The cuticle at the apex of the dome is about 0.7 μm thick but thins abruptly to about 0.4 μm along the lateral sides. In glands fixed by chemical methods, the essential oil is preserved as a moderately densely staining material that fills most of the sub-cuticular space (Fig. 7A). As before, a fibrillar material coats the glandular disc cells, thus separating them from the stored essential oil (Fig. 7A).

Post-secretory glandular disc cells are vacuolate, with large central vacuoles that contain an evenly dispersed fibrillar material (Fig. 7B). The thin radial walls of the glandular disc cells are often highly folded in chemically fixed specimens but such extensive wall folding and distortion of cell shape is not encountered with cryofixation (Fig. 7B). The peripheral cytoplasm contains moderately developed SER and mitochondria are abundant (Fig. 7D). Polysomes are present and are both attached to short segments of ER and free in the cytoplasm. Golgi are also present, but uncommon. Disc cells contain nuclei with heterochromatin and small nucleoli (Fig. 7C). The plastidome is much less conspicuous than in secretory stage glands. The plastids are relatively small, variable in shape, occasionally contain large plastoglobuli, and often have prominent tubular internal membranes along the periphery (Fig. 7E).

The stalk cell of post-secretory glands retains its original diameter tangentially but becomes radically narrow (Fig. 7A). The cell wall appears thicker than that of a secretory phase stalk cell, yet still contains plasmodesmata. The post-secretory stalk cell has numerous mitochondria, microbodies, and large plastids. The plastids are usually oblong and contain large plastoglobuli (Fig. 7F).

The post-secretory basal cell is similar to the basal cell of secretory stage glands because it contains a large central vacuole, abundant mitochondria, abundant SER, and an intact nucleus, occasionally with a moderately large nucleolus. Cell walls of post-secretory stage basal cells appear thicker than those of previous stages, but maintain numerous branched plasmodesmata. These cells also differ from basal cells of the previous stages in that they consistently contain large lipid-filled vesicles in the peripheral cytoplasm (Fig. 7, G–I). In addition, microbodies with large paracrystalline inclusions are occasionally encountered in these cells.

DISCUSSION

Remarkable ultrastructural transformations occur at the onset of secretion in the peltate glands of peppermint that correlate with the peak of monoterpene production in developing leaves (Turner et al., 1999, 2000; Gershenzon et al., 2000; McConkey et al., 2000) and suggest possible roles for both leucoplasts and SER in monoterpene biosynthesis and export. These changes include the formation of a large subcuticular secretion storage space above the gland disc cells and the development of extensive SER (containing lipid) and the enlargement of leucoplasts in these secretory cells. The glandular stalk cells also undergo intriguing modifications correlated with secretory activity. These alterations include the development of distinctive plastids, numerous microbodies, and abundant mitochondria. It is interesting that the prolamellar body-like membranes of stalk cell plastids somewhat resemble structures that develop within secretory phase disc cell leucoplasts of *Cannabis sativa* (Kim and Mahlberg, 1997) as well as membrane aggregations seen in plastids of soybean glandular trichomes (Franceschi and Giaquinta, 1983). The abundant microbodies suggest active oxidative metabolism. Because the cuticle and suberized lateral walls are fully developed prior to the secretory phase, it is unlikely that stalk cells are specialized for cutin synthesis. It is likely that at least some of the specializations of these cells are related to their essential role in the supply of carbon substrates to the non-photosynthetic disc cells during the brief but intense period of secretion.

Most previous investigations of Lamiaceae gland ultrastructure have described the apparent senescence of disc cells immediately after the secretory phase of development (Amelunxen, 1965; Bosabalidis and Tsekos, 1982; Ascensão et al., 1997). Mature, oil-filled glands are very difficult to preserve by stan-

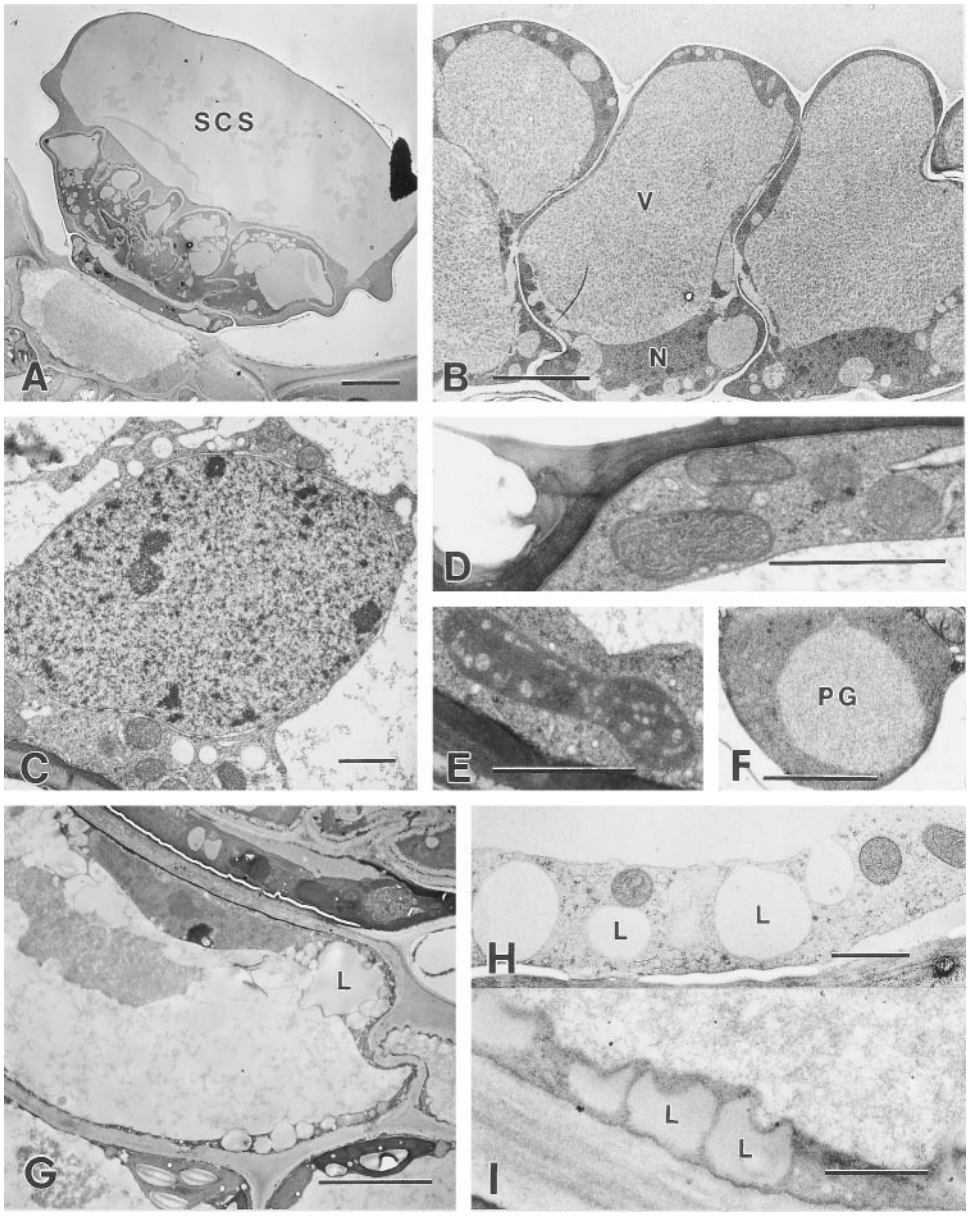

Figure 7. Post-secretory stage. A, Chemically fixed post-secretory stage peltate gland showing a large SCS containing lipid above the fibrillar material coating the glandular disc cells. Bar = 10 μm. B, Cryofixed glandular disc cells from a post-secretory phase peltate gland. The cell walls show less distortion than those of post-secretory stage glands prepared by chemical fixation. The cells contain nuclei (N), mitochondria, and large central vacuoles (V). Bar = 5 μm. C, Typical nucleus from a cryofixed glandular disc cell containing heterochromatin and lacking well-developed nucleoli. Bar = 1 μm. D, Mitochondria adjacent to the sub-cuticular space of a cryofixed post-secretory glandular disc cell. Bar = 1 μm. E, Typical plastid from a cryofixed post-secretory glandular disc cell that is smaller than the large leucoplasts of secretory stage glands. Bar = 1 μm. F, Cryofixed stalk cell plastid with large plastoglobule (PG). Bar = 1 μm. G, Chemically fixed basal cell of a post-secretory stage peltate gland. The peripheral cytoplasm contains numerous lipid spherosomes (L). Bar = 5 μm. H, Cryofixed peripheral cytoplasm of a post-secretory gland basal cell showing vacuole-like structures (L) that correspond to lipid spherosomes of chemically fixed specimens. Compare with (I). Bar = 1 μm. I, Peripheral cytoplasm showing lipid spherosomes (L) of a chemically fixed post-secretory gland basal cell. Compare with (H). Bar = 1 μm.

dard methods; however, the secretory disc cells of post-secretory stage glands prepared by cryofixation contain intact organelles and appear to be living. Although both in vivo and enzyme-level analyses have shown that post-secretory glands are no longer active in monoterpene production, the secretory cells nevertheless carry out substantial reductive metabolism in the conversion of menthone to the principal essential oil component menthol (Gershenzon et al., 2000; McConkey et al., 2000; Turner et al., 2000).

Enlargement of the Sub-Cuticular Space

The way in which the sub-cuticular space is formed, and the possibility that the cuticle is reinforced during expansion by additional cutin deposition, have been the subject of some debate. The initial cuticular separation from the disc cells leaves a thin residual cell wall layer of consistent thickness on the cuticle. Similar residual wall layers have been found on the oil gland cuticles of other Lamiaceae species (Bourett et al., 1994; Ascensão et al., 1997). These observations suggest that the cuticle-wall separation occurs at a predetermined zone of weakness. Therefore, the gland cuticles of the Lamiaceae family appear to be comparable to the wall-cuticle dermal sheaths of *C. sativa* glandular trichomes (Kim and Mahlberg, 1991), although the residual wall in *Cannabis* is much thicker.

The source of cutin for the expanding cuticle of Lamiaceae oil glands has been uncertain. Several authors have noted that the cuticle remains relatively thick during expansion or that it even appears to become thicker with age. Both Amelunxen (1965), based on studies with peppermint, and Bosabalidis and Tsekos (1982), based on studies with *Origanum*, advocated the hypothesis that new cutin is added to the expanding cuticle at the base where it attaches to the stalk cell. Kim and Mahlberg (1995) proposed that in *Cannabis* (Cannabaceae) glands, vesicle-like structures within the sub-cuticular space carry deposits of cutin to the expanding cuticle. No evidence to support either of these complex dynamic proposals was obtained with peppermint glands. Rather, it was shown that during expansion of the sub-cuticular space, the gland cuticle becomes thinner along the lateral sides while the central region of the dome remains thick. Cuticles of glands from late presecretory and secretory stages have cuticles of near-identical thickness at the gland apex (about 0.7 μm), and the lateral sides appear thinner in post-secretory stages. Thus it appears that the cutin polymer of early-stage secretory glands is sufficiently thick and flexible to accommodate the plastic deformation necessary to reach full expansion without requiring additional synthesis.

Two different secreted materials are evident in the newly formed sub-cuticular space of early secretory stage glands. The nascent, and still small, sub-cuticular space appears to be filled mostly with an opaque fibrillar material. Lipid secretion appears first as small pools of lipid within this fibrillar substance, which is apparently hydrophilic. Similar materials were described in expanding glandular sub-cuticular spaces of the oil glands of *Leonotis leonurus* (Ascensão et al., 1997), *Origanum* × *intercedens* (Bosabalidis et al., 1998), and *Salvia glutinosa* (Schnepf, 1972). Ascensão et al. (1997) interpreted the fibrillar substance as loosened cell wall components and used histochemical stains to show that it contained carbohydrate. However, in cryogenically fixed and microwave-fixed peppermint gland specimens, the fibrillar material appears clearly distinct from the walls. Since monoterpenes can be toxic to plant cells (Shomer and Erner, 1989; Loveys et al., 1992), the hydrophilic material could represent a protective mucilage-containing barrier between the secreted oil and the glandular cap cells. Histochemical staining has shown that, in addition to lipids which form the bulk of the stored secretion, the peltate glands of *Salvia aurea* (Serrato-Valenti et al., 1997), *Salvia blepharophylla* (Bisio et al., 1999), and *O. intercedens* (Bosabalidis et al., 1998) also contain non-cellulosic carbohydrates as well as phenolic material. The secretion of peppermint peltate glands consists mostly of monoterpenes but also contains abundant flavone aglycones (Vorin and Bayet, 1992; Vorin et al., 1993), and it is possible that some of the ultrastructural features described here may represent specializations for the secretion of these flavonoid products. Recent evidence suggests that a number of flavonoid and phenylpropanoid biosynthetic enzymes are clustered at the ER (Burbulis and Winkel-Shirley, 1999; Winkel-Shirley, 1999).

Site of Monoterpene Biosynthesis and Possible Secretory Mechanisms

Many previous investigators have noted similar ultrastructural features of oil and resin gland secretory cells from taxonomically distant plants, including amoeboid leucoplasts, an abundance of smooth SER, numerous mitochondria, and relatively few Golgi. Often the cytoplasm of the secretory cells was reported to be densely stained, with lipid deposits in ER and plastids as well as cytoplasmic droplets (Amelunxen, 1965; Schnepf, 1974; Dell and McComb, 1978; Heinrich et al., 1983; Ascensão et al., 1997). These observations have led to a range of speculations concerning the possible sites of terpenoid synthesis and the possible mechanisms of oil secretion. In particular for Lamiaceae oil glands, these proposals have included cytoplasmic synthesis and eccrine secretion (Bosabalidis and Tsekos, 1982), synthesis in vacuoles (Amelunxen, 1965) or SER (Schnepf, 1972), synthesis in plastids associated with SER and with oil transport by an unknown process (Bourett et al., 1994), and synthesis in plastids with involvement of SER in the transport of the terpenoid secretion (Ascensão et al., 1997). Early speculations were based largely upon observations of the apparent sites of lipid accumulation during the secretory phase of development. Since leucoplasts in secretory phase glandular disc cells of mints generally lack lipid deposits, most early reports focused on other cytoplasmic features.

There is now ample evidence to indicate that monoterpene synthesis from primary metabolism is initiated within leucoplasts. This evidence includes the correlation between the production of monoterpene secretion products and the presence of amoe-

boid leucoplasts in the corresponding secretory cells (Cheniclet and Carde, 1985), the biosynthesis of unmodified monoterpenes by isolated leucoplasts (Pauly et al., 1986; Soler et al., 1992), and the documented origin of monoterpenes by the nonmevalonate pathway (Eisenreich et al., 1997; Sagner et al., 1998) that is known to be localized in plastids (Eisenreich et al., 1998; Lichtenthaler, 1999). In addition, both geranyl diphosphate synthase, which catalyzes the condensation of the primary metabolites isopentenyl diphosphate and dimethylallyl diphosphate to the acyclic precursor of monoterpenes, and (−)-limonene synthase, which catalyzes the first dedicated step of monoterpene biosynthesis in peppermint, are encoded as preproteins bearing N-terminal plastidial targeting sequences (Colby et al., 1993; Burke et al., 1999). The plastid import and processing of limonene synthase and the immunocytochemical localization of this enzyme in peppermint secretory cell leucoplasts have also been demonstrated recently (Turner et al., 1999).

Other evidence suggests an important role for SER in monoterpene biosynthesis. In peppermint and spearmint, the subsequent hydroxylations of plastid-derived limonene to form (−)-trans-isopiperitenol (in peppermint) and (−)-trans-carveol (in spearmint) are carried out by cytochrome P450 limonene 3- and 6-hydroxylases, respectively. These enzymes are considered to be ER-resident proteins because they bear typical N-terminal membrane insertion sequences (Lupien et al., 1999) and they are localized exclusively in the microsomal fraction of oil gland extracts (Karp et al., 1990). However, further steps in the metabolism to menthol in peppermint (Fig. 1) are carried out by operationally soluble redox enzymes (Croteau et al., 1991), and recent evidence (M. McConkey, E. Davis, and R. Croteau, unpublished data) indicates that the cDNAs encoding several of the pathway reductases are translated without any apparent N-terminal targeting information, indicating probable cytosolic proteins.

Abundant SER is a common feature of lipid-secreting glandular cells (Amelunxen, 1965). The extensive elaboration of SER in disc cells of peppermint peltate glands during the secretory phase, the very close association with leucoplasts and the plasma membrane, and the presence of lipid deposits within the SER strongly suggest that SER has an additional role in transport and secretion of monoterpenes to the storage cavity. The close association of SER with secretory cell leucoplasts could facilitate transfer of monoterpenes from the plastids to ER, and the very close approach of lipid-filled SER to the plasma membrane suggests a role in the export of monoterpenes from the secretory cells to the storage space. It is probable that transport of monoterpenes from one subcellular compartment to another and the eventual secretion against the concentration gradient of the storage compartment would require a number of specialized lipid carrier and transfer proteins.

Robards and Stark (1988) described similar extensive SER in cryofixed nectary cells of *Abutilon* and postulated a secretion mechanism for *Abutilon* nectar mediated by direct SER-plasma membrane connections. It is tempting to propose a similar secretion model for mint essential oil involving initial biosynthesis of limonene in plastids, followed by modification at and transport via SER to the plasma membrane for export by an active transport process. However, since the final steps in monoterpene metabolism involve redox transformations catalyzed by ostensibly cytosolic enzymes, this model can apply only if these enzymes associate with the secretory membrane systems or SER, or if these highly lipophilic metabolites are trafficked between ER and cytosolic sites of metabolism by carrier proteins. Such complex intracellular trafficking of isoprenoid metabolites is known to occur, for example, in the biosynthesis of some mammalian steroids in which initial steps occur in mitochondria, intermediate steps involve ER resident enzymes, and final steps occur again in mitochondria (Miller, 1988; Black et al., 1994; Ishimura and Fujita, 1997; Staehelin, 1997). Further elucidation of the organization of monoterpene metabolism and of the mechanism of oil secretion will require characterization and immunocytochemical localization of the biosynthetic enzymes and of the transport proteins involved.

MATERIALS AND METHODS

Peppermint (*Mentha* × *piperita* L. cv Black Mitcham) plants were propagated from rhizomes and grown in a controlled environment as described in detail elsewhere (Gershenzon et al., 2000). Specimens of this material for HPFS were processed at the Center for Electron Microscopy (Biology Department, University of Memphis, TN). Immediately prior to freezing, 1-mm^2 samples were dissected from leaves of 4-week-old shoots and placed in Balzers high pressure freezer specimen sandwiches (Ted Pella, Redding, CA) with either hexadecene or buffered 0.2 M-Suc to exclude air. Samples were rapidly frozen with double jets of pressurized liquid nitrogen using a Balzers high pressure freezing machine (HPM 010). Some specimens were then freeze substituted for 72 h at −90°C in dry HPLC-grade acetone (Fisher, Atlanta), which contained 2% (w/v) OsO_4 in a Balzers freeze-substitution unit (FSU 010) and was then gradually warmed to room temperature prior to embedding in epon resin. Other specimens were freeze-substituted at −90°C in dry acetone with 2% (w/v) OsO_4 and 1% (w/v) uranyl acetate. These specimens remained in this solution at −60°C for 16 h before being gradually warmed to room temperature, rinsed in acetone, and embedded in epon resin.

Similar 1-mm^2 samples were dissected from leaves of 4-week-old-shoots for rapid microwave and slow (overnight) chemical fixation. The samples included leaves of all

developmental ages, ranging from small primordia to fully expanded, mature leaves. Some samples (chemical fixed) were fixed with 3% (v/v) glutaraldehyde and 0.1% (w/v) OsO_4 in 0.05 M 1,4-piperazinediethanesulfonic acid (PIPES) (pH 7.2) buffer for 2 h in an ice bath followed by rinses with 0.05 M PIPES buffer. These specimens were then transferred to a similar 3% (v/v) glutaraldehyde solution that lacked OsO_4. After 12 h, samples were postfixed with 1% (w/v) OsO_4 in 0.05 M PIPES buffer (pH 7.2) for 2 h at 4°C. Buffered rinses were made between each treatment.

Additional specimens (microwave fixed) were rapidly fixed and dehydrated using a solution of 3.5% (v/v) glutaraldehyde and 0.05% (w/v) OsO_4 (buffered with 0.05 M PIPES, pH 7.2) for 2.5 min at 37°C in a Pelco model 3450 tissue processing microwave oven (Ted Pella, Redding, CA). After buffer rinses, the specimens were postfixed for 5 min at 37°C in 1% (w/v) OsO_4, rinsed with buffer, rapidly dehydrated in the microwave oven with a graded ethanol or acetone series at 40°C, and then infiltrated with EMbed-812 resin (Electron Microscopy Sciences, Fort Washington, PA).

HPFS provided the best preservation of organellar membranes; however, the low-M_r lipids within the cells and within the SCS were extracted during freeze-substitution with acetone. Much of this easily solubilized material is presumably essential oil. Heinrich (1970) identified similar material from *Poncirus* glands as essential oil because it was volatilized and lost during freeze-drying. Therefore, determination of the distribution of these lipids within the glandular cells required standard chemical fixation. Rapid microwave fixation proved to be the most suitable of the chemical fixation methods in providing excellent ultrastructural preservation and lipid retention.

Sections for light microscopy were cut to a thickness of 0.5 to 1 μm with glass knives and stained with toluidine blue. Specimens were viewed with a light microscope (model BH-2, Olympus, Tokyo). Sectioning for electron microscopy was accomplished with a diamond knife (Diatone U.S., Fort Washington, PA) and an Ultracut R ultramicrotome (Leica Microsystems, Wetzlar, Germany). Silver sections for electron microscopy were collected on carbon-formvar-coated grids or uncoated mesh grids. Most sections were stained with either 2% (w/v) aqueous uranyl acetate and 1% (w/v) lead citrate or with a uranyl acetate-$KMnO_4$ solution consisting of 3 parts of 2% (w/v) aqueous uranyl acetate and 1 part of 1% (w/v) aqueous $KMnO_4$ that was mixed and filtered immediately prior to staining (Franceschi et al., 1994). Some specimens were stained for 15 min with a 1% (w/v) phosphotungstinate solution (pH 7.3). Stained sections were viewed with an H-600 (Hitachi, Tokyo) or a JEM 1200EX (JEOL, Tokyo) electron microscope and photographed with electron microscopy film (Eastman-Kodak, Rochester, NY).

We used a Pulnix TM-7 CCD camera (Pulnix America, Sunnyvale, CA) mounted on a copy stand, a Quadra 950 (Apple Computer, Cupertino, CA), and NIH Image (version 1.60, developed at the U.S. National Institutes of Health and available on the Internet at http://rsb.info.nih.gov/nih-image) to capture digitized images of printed micrographs of known magnification to measure the cuticle thickness of glandular trichomes.

ACKNOWLEDGMENTS

We thank Howard Berg for assistance with high-pressure freezing and freeze substitution, Vincent Franceschi for helpful discussions, the staff of the Electron Microscopy Center at Washington State University for technical support, Massimo Maffei for assistance in the early phase of this study, Thom Koehler for raising the plants, and Joyce Tamura for typing the manuscript.

Received February 2, 2000; accepted June 1, 2000.

LITERATURE CITED

Amelunxen F (1965) Elektronenmikroskopische Untersuchungen an den Drüsenschuppen von *Mentha piperita* L. Plant Med **13:** 457–473

Ascensão L, Marques N, Pais MS (1997) Peltate glandular trichomes of *Leonotis leonurus* leaves: ultrastructure and histochemical characterization of secretions. Int J Plant Sci **158:** 249–258

Bisio A, Corallo A, Gastaldo P, Romussi G, Ciarallo G, Fontana N, De Tommasi N, Profumo P (1999) Glandular hairs and secreted material in *Salvia blepharophylla* Brandegee ex Epling grown in Italy. Ann Bot **83:** 441–452

Black SM, Harikrishna JA, Szklarz GD, Miller WL (1994) The mitochondrial environment is required for the activity of the cholesterol side-chain cleavage enzyme, cytochrome P450scc. Proc Natl Acad Sci USA **91:** 7247–7251

Bosabalidis A, Gabrieli C, Niopas I (1998) Flavone aglycones in glandular hairs of *Origanum* × *intercedens*. Phytochemistry **49:** 1549–1553

Bosabalidis A, Tsekos I (1982) Glandular scale development and essential oil secretion in *Origanum dictamnus* L. Planta **156:** 496–504

Bourett TM, Howard RJ, O'Keefe DP, Hallahan DL (1994) Gland development on leaf surfaces of *Nepeta racemosa*. Int J Plant Sci **155:** 623–632

Burbott AJ, Loomis WD (1967) Effects of light and temperature on the monoterpenes of peppermint. Plant Physiol **42:** 20–28

Burbulis IE, Winkel-Shirley B (1999) Interactions among enzymes of the *Arabidopsis* flavonoid biosynthetic pathway. Proc Natl Acad Sci USA **96:** 12929–12934

Burke C, Wildung MR, Croteau R (1999) Geranyl diphosphate synthase: cloning, expression and characterization of this prenyltransferase as a heterodimer. Proc Natl Acad Sci USA **96:** 13062–13067

Cheniclet C, Carde J-P (1985) Presence of leucoplasts in secretory cells and of monoterpenes in the essential oil: a correlative study. Isr J Bot **34:** 219–238

Clark RJ, Menary RC (1980) Environmental effects on peppermint (*Mentha piperita* L.): I. Effect of daylength,

photon flux density, night temperature and day temperature on the yield and composition of peppermint oil. Aust J Plant Physiol **7:** 685–692

Colby SM, Alonso WR, Katahira EJ, McGarvey DJ, Croteau R (1993) 4*S*-Limonene synthase from the oil glands of spearmint (*Mentha spicata*): cDNA isolation, characterization and bacterial expression of the catalytically active monoterpene cyclase. J Biol Chem **268:** 23016–23024

Croteau R, Gershenzon J (1994) Genetic control of monoterpene biosynthesis in mints (*Mentha*:Lamiaceae). Recent Adv Phytochem **28:** 193–229

Croteau R, Karp F, Wagschal KC, Satterwhite DM, Hyatt DC, Skotland CB (1991) Biochemical characterization of a spearmint mutant that resembles peppermint in monoterpene content. Plant Physiol **96:** 744–752

Dell B, McComb AJ (1978) Plant resins: their formation, secretion, and possible functions. Adv Bot Res **6:** 277–316

Eisenreich W, Sagner S, Zenk MH, Bacher A (1997) Monoterpenoid essential oils are not of mevalonoid origin. Tetrahedron Lett **38:** 3889–3892

Eisenreich W, Schwarz M, Cartayrade A, Arigoni D, Zenk MH, Bacher A (1998) The deoxyxylulose phosphate pathway of terpenoid biosynthesis in plants and microorganisms. Chem Biol **5:** R221–R223

Franceschi VR, Ding B, Lucas WJ (1994) Mechanism of plasmodesmata formation in characean algae in relation to evolution of intercellular communication in higher plants. Planta **192:** 347–358

Franceschi VR, Giaquinta RT (1983) Glandular trichomes of soybean leaves: cytological differentiation from initiation through senescence. Bot Gaz **144:** 175–184

Galway ME, Heckman JW, Hyde GJ, Fowke LC (1995) Advances in high-pressure and plunge-freeze fixation. Methods Cell Biol **49:** 3–19

Gershenzon J, Maffei M, Croteau R (1989) Biochemical and histochemical localization of monoterpene biosynthesis in the glandular trichomes of spearmint (*Mentha spicata*). Plant Physiol **89:** 1351–1357

Gershenzon J, McCaskill D, Rajaonarivony JIM, Mihaliak C, Karp F, Croteau R (1992) Isolation of secretory cells from plant glandular trichomes and their use in biosynthetic studies of monoterpenes and other gland products. Anal Biochem **200:** 130–138

Gershenzon J, McConkey M, Croteau R (2000) Regulation of monoterpene accumulation in leaves of peppermint (*Mentha* × *piperita* L). Plant Physiol **122:** 205–213

Giberson RT, Demaree RS Jr, Nordhausen RW (1997) Four-hour processing of clinical/diagnostic specimens for electron microscopy using microwave techniques. J Vet Diagn Invest **9:** 61–67

Hayat MA (1989) Principles and Techniques of Electron Microscopy, Ed 3. CRC Press, Boca Raton, FL

Heinrich G (1970) Elektronenmikroskopische Beobachtungen an den Drüsenzellen von *Poncirus trifoliata*; zugleich ein Beitrag zur Wirkung ätherischer Öle auf Pflanzenzellen und eine Methode zur Unterscheidung flüchtiger von nichtflüchtigen lipophilen Komponenten. Protoplasma **69:** 15–36

Heinrich G, Schultze W, Pfab I, Böttger M (1983) The site of essential oil biosynthesis in *Poncirus trifoliata* and *Monarda fistulosa*. Physiol Veg **21:** 257–268

Ishimura K, Fujita H (1997) Light and electron microscopic immunohistochemistry of the localization of adrenal steroidogenic enzymes. Microsc Res Tech **36:** 445–453

Karp F, Mihaliak CA, Harris JL, Croteau R (1990) Monoterpene biosynthesis: specificity of the hydroxylations of (−)-limonene by enzyme preparations from peppermint (*Mentha piperita*), spearmint (*Mentha spicata*), and perilla (*Perilla frutescens*) leaves. Arch Biochem Biophys **276:** 219–226

Kim E-S, Mahlberg PG (1991) Secretory cavity development in glandular trichomes of *Cannabis sativa* L (Cannabaceae). Am J Bot **78:** 220–229

Kim E-S, Mahlberg PG (1995) Glandular cuticle formation in *Cannabis* (Cannabaceae). Am J Bot **82:** 1207–1214

Kim E-S, Mahlberg PG (1997) Plastid development in disc cells of glandular trichomes of *Cannabis* (Cannabaceae). Mol Cell **7:** 352–359

Kjonaas R, Croteau R (1983) Demonstration that limonene is the first cyclic intermediate in the biosynthesis of oxygenated *p*-menthane monoterpenes in *Mentha piperita* and other *Mentha* species. Arch Biochem Biophys **220:** 79–89

Kjonaas R, Martinkus-Taylor C, Croteau R (1982) Metabolism of monoterpenes: conversion of *l*-menthone to *l*-menthol and *d*-neomenthol by stereospecific dehydrogenases from peppermint (*Mentha piperita*) leaves. Plant Physiol **69:** 1013–1017

Lichtenthaler HK (1999) The 1-deoxy-D-xylulose-5-phosphate pathway of isoprenoid biosynthesis in plants. Annu Rev Plant Physiol Plant Mol Biol **50:** 47–66

Loveys BR, Robinson SP, Brophy JJ, Chacko EK (1992) Mango sapburn: components of fruit sap and their role in causing skin damage. Aust J Plant Physiol **19:** 449–457

Lupien S, Karp F, Wildung M, Croteau R (1999) Regiospecific cytochrome P450 limonene hydroxylases from mint (*Mentha*) species: cDNA isolation, characterization, and functional expression of (−)-4*S*-limonene-3-hydroxylase and (−)-4*S*-limonene-6-hydroxylase. Arch Biochem Biophys **368:** 181–192

McCaskill D, Gershenzon J, Croteau R (1992) Morphology and monoterpene biosynthetic capabilities of secretory cell clusters isolated from glandular trichomes of peppermint (*Mentha piperita* L.). Planta **187:** 445–454

McConkey M, Gershenzon J, Croteau R (2000) Developmental regulation of monoterpene biosynthesis in the glandular trichomes of peppermint (*Mentha* × *piperita* L.). Plant Physiol **122:** 215–223

Mihaliak CA, Gershenzon J, Croteau R (1991) Lack of rapid monoterpene turnover in rooted plants: implications for theories of plant chemical defense. Oecologia **87:** 373–376

Miller WL (1988) Molecular biology of steroid hormone synthesis. Endocr Rev **9:** 295–318

Parthasarathy MV (1995) Freeze-substitution. Methods Cell Biol **49:** 57–69

Pauly G, Belingheri L, Marpeau A, Gleizes M (1986) Monoterpene formation by leucoplasts of *Citrofortunella*

mitis and *Citrus unshiu*: steps and conditions of biosynthesis. Plant Cell Rep **5:** 19–22

Robards AW, Stark M (1988) Nectar secretion in *Abutilon*: a new model. Protoplasma **142:** 79–91

Sagner S, Latzel C, Eisenreich W, Bacher A, Zenk MH (1998) Differential incorporation of 1-deoxy-D-xylulose into monoterpenes and carotenoids in higher plants. J Chem Soc Chem Commun 221–222

Schnepf E (1972) Tubuläres endoplasmatisches Reticulum in Drüsen mit lipophilen Ausscheidungen von *Ficus*, *Ledum*, und *Salvia*. Biochem Physiol Pflanz **163:** 113–125

Schnepf E (1974) Gland cells. *In* AW Robards, ed, Dynamic Aspects of Plant Ultrastructure. McGraw-Hill, London, pp 331–357

Serrato-Valenti G, Bisio A, Cornara L, Ciarallo G (1997) Structural and histochemical investigation of the glandular trichomes of *Salvia aurea* L. leaves, and chemical analysis of the essential oil. Ann Bot **79:** 329–336

Shomer I, Erner Y (1989) The nature of oleocellosis in citrus fruits. Bot Gaz **150:** 281–288

Soler E, Feron G, Clastre M, Dargent R, Gleizes M, Ambid C (1992) Evidence for a geranyl diphosphate synthase located within plastids of *Vitis vinifera* L. cultivated in vitro. Planta **187:** 171–175

Staehelin AL (1997) The plant ER: a dynamic organelle composed of a large number of discrete functional domains. Plant J **11:** 1151–1165

Turner GW, Gershenzon J, Croteau RB (2000) Distribution of peltate glandular trichomes on developing leaves of peppermint. Plant Physiol **124:** 655–663

Turner GW, Gershenzon J, Nielson EE, Froehlich JE, Croteau RB (1999) Limonene synthase, the enzyme responsible for monoterpene biosynthesis in peppermint, is localized to leucoplasts of oil gland secretory cells. Plant Physiol **120:** 879–886

Vorin B, Bayet C (1992) Developmental variations in leaf flavonoid aglycones of *Mentha* × *piperita*. Phytochemistry **31:** 2299–2304

Vorin B, Bayet C, Colson M (1993) Demonstration that flavone aglycones accumulate in the peltate glands of *Mentha* × *piperita* leaves. Phytochemistry **34:** 85–87

Winkel-Shirley B (1999) Evidence for enzyme complexes in the phenylpropanoid and flavonoid pathways. Physiol Plant **107:** 142–149

Wise ML, Croteau R (1999) Monoterpene biosynthesis. *In* DE Cane, ed, Comprehensive Natural Products Chemistry, Vol 2, Isoprenoids Including Carotenoids and Steroids. Elsevier Science, Oxford, pp 97–153